Generation and Validation of di-Higgs events in the 4τ final state

Uppsala University
Department Of Physics and Astronomy

Project Course, 15 c

Author: Halimeh Vaheid
Supervisor: Arnaud Ferrari

UPPSALA
UNIVERSITET

Contents

1 Introduction

1.1 The Standard Model

The *Standard Model* (SM) is a theory of particle physics describing the strong, electromagnetic and weak interactions of elementary particles in a quantum field theory framework. It contains three generations of fermions whose interactions are mediated by *gauge bosons* (see Fig. 1). The electromagnetic force is carried by the photon while Z and W bosons mediate the weak interaction [1, 2]. The gluons are the force carriers of the strong interaction. The SM has predicted a wide range of experimental observations. One of them is the *Higgs* boson, h, whose existence used to be the last unverified part of the SM. On the 4th July 2012, scientists of *ATLAS* [3] and *CMS* [4] at CERN confirmed the observation of a Higgs-like boson with a mass of 125 GeV [5, 6].

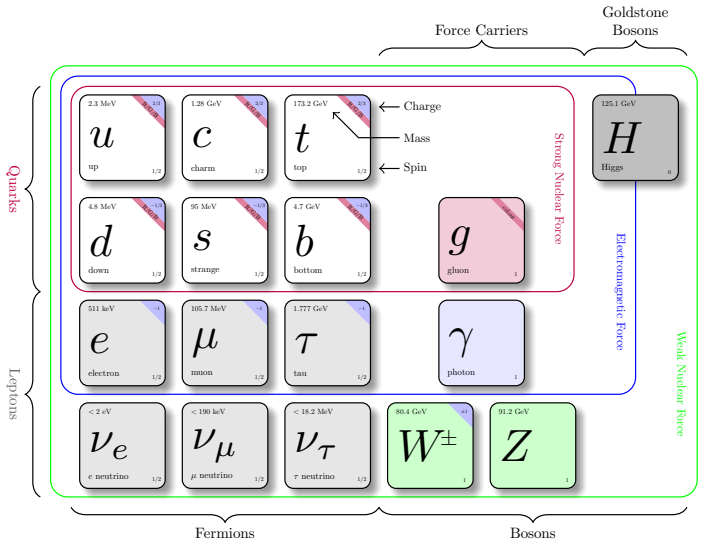

Figure 1: The fundamental particles of the SM.

1.2 The Higgs Boson

The Higgs boson is an elementary particle resulting from the quantum excitation of the Higgs field. Both fermions and gauge bosons gain mass through the interaction with a Higgs field in a local gauge invariance theory [7]. In the SM, the mass of the Higgs particle is a free parameter, but given its mass one can determine many parameters like the Higgs *self-coupling*, λ, and the Higgs scalar field potential. The Higgs self-coupling is the matter of interest because it is connected to the potential which results from the spontaneous symmetry breaking of electroweak interaction. In the SM, one can determine the potential using a single Higgs self-coupling, $V_{SM} = -\mu^2\phi^\dagger\phi + \lambda|\phi^\dagger\phi|^2$. The Higgs mass is proportional to the square root of λ, $M_h = \sqrt{\lambda}v$ where v is the vacuum expectation value of the Higgs field. The measured value of $M_h = 125$ GeV implies that $\lambda_{SM} = 0.26$ [8].

The Higgs trilinear self-coupling, λ_{hhh}, not only gives information about the shape of the scalar potential, but it also affects the value of the Higgs pair production cross section. In addition, probing λ_{hhh} might indicate physics beyond the SM (BSM).

2 Theoretical Background

2.1 Higgs Mechanism

All basic equations coming from the unified electroweak theory correctly describe the electroweak force and its associated force-carriers, namely the photon, and the W and Z bosons, except for a major glitch. While only the photon is massless in reality, all other force-carrying particles emerge also without mass in the theory. Fortunately, this problem was solved by Peter Higgs, Robert Brout and Francois Englert when they introduced the *Brout-Englert-Higgs (BEH) mechanism*, which requires the implementation of a scalar doublet. The dimensionless Higgs coupling constant allows the Higgs field to have a non-zero vacuum expectation value (VEV). Through the coupling of Higgs doublet with the other SM fields, the aforementioned VEV gives mass to other SM particles including W and Z bosons. Therefore, a consequence of the existence of the Higgs particle and its self-couplings is electroweak symmetry breaking (EWSB). The actual measurement of the Higgs self-coupling would help us to confirm the EWSB and know to what extent the electroweak symmetry is broken [9, 10].

2.2 Higgs Pair Production

The production of Higgs pairs at hadron colliders not only gives information on the Higgs sector but also on the BEH mechanism. It results in several types of final states, with probabilities given by the branching decays of each Higgs boson in the pair. One way of producing a Higgs boson pair is via Higgs self-coupling. Other interactions like the Higgs–fermion Yukawa interactions may also yield to the Higgs pair. Fig. 2 shows the Leading Order (LO) Feynman diagrams for the SM Higgs pair production. The LO means that all vertices in the Feynman diagrams emerge from the *lowest-order-Lagrangian*. All terms in the lowest-order-Lagrangian are at most of order Q^2 in the Taylor expansion of the typical momentum scale Q. Consequently, all vertices of LO Feynman diagrams contribute at order Q^2 in the *Feynman matrix*. The triangle diagram is sensitive to the Higgs self-coupling. The destructive interference of the box-like with the triangle diagram results in a small cross section for di-Higgs production. The prediction of the SM for the Higgs pair production cross section is $\sigma_{hh} = 33.49$ fb [11]. The dominant process to produce a Higgs pair is gluon-gluon fusion. Although the cross section of the other pair production channels, like the vector-boson fusion channel, is at least one order of magnitude smaller, they are still interesting due to the different sensitivity to λ or to new physics [12].

2.3 Higgs Decay Modes

Fig. 3 shows how the branching ratios depend on the mass of the Higgs particle. The Higgs particle does not decay to light quarks and the branching ratio for the Higgs decay to two photons is very small. The SM Higgs decays to a pair of heavy quarks or gauge bosons with a high probability.

In this project, we are going to consider $hh \to \tau\tau\tau\tau$. The branching ratio for the SM Higgs boson decaying to 2τ is 6.4%, therefore the total branching ratio of our decay channel is 0.41%.

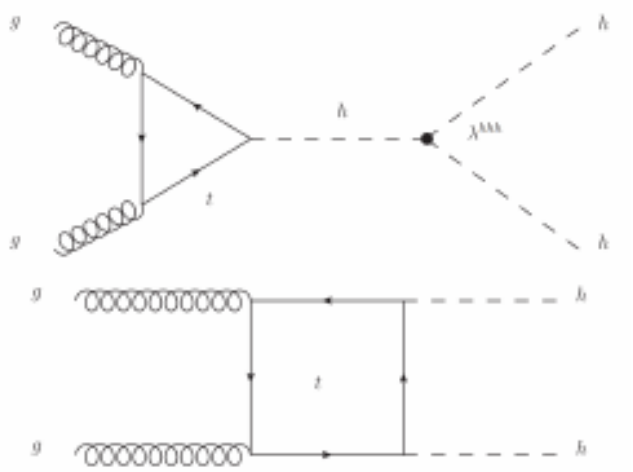

Figure 2: LO Feynman diagrams of di-Higgs production via gluon-gluon fusion. The upper diagram is sensitive to the trilinear Higgs boson self-coupling. The box-like diagram reduces the sensitivity because it interferes with the triangle diagram destructively [11].

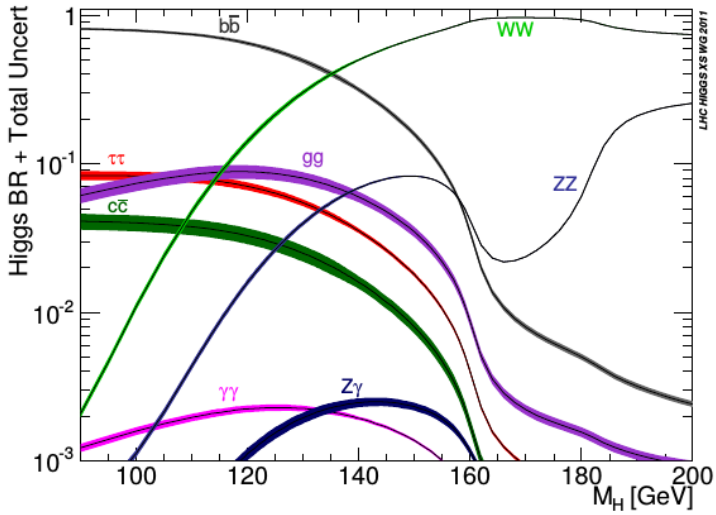

Figure 3: Decay branching ratios as a fraction of the mass of Higgs particle [13].

2.4 τ Decay Modes

The τ is the heaviest lepton with a mass of 1.78 GeV/c^2. Its life-time is 1.3×10^{-13} s and it decays either hadronically or leptonically through the weak interaction by mediating a W boson. The τ is the only lepton which is heavy enough to decay into hadrons. There is always a ν_τ in the decay products of τ. Table 1 shows different τ decay channels with their corresponding branching ratios [14].

Decay mode	Branching ratio%
$e\nu_e\nu_\tau$	17.85
$\mu\nu_\mu\nu_\tau$	17.36
$q\bar{q}\nu_\tau$	64.70

Table 1: The branching ratios of τ decays.

3 Framework

3.1 Relativistic Kinematics

All particles involved in a high energy physics experiment are relativistic and their energies and momenta are expressed in a four-vector formalism, $p^{\mu}(\mu = 0, 1, 2, 3,)$. The four-momentum conservation, the invariant mass, and generally the kinematics of all involved particles give practical information about the reaction of interest and the properties of the initial and final particles. The invariant mass is defined as

$$M^2 = E^2 - |\vec{P}|^2 = p_{\mu}p^{\mu} \tag{1}$$

where p^{μ} and p_{μ} are contravariant and covariant four-vectors respectively, which are related to each other through the Minkowski metric $g^{\mu\nu}$ with the signature $(+, -, -, -)$

$$p^{\mu} = (E, \vec{p}) = g^{\mu\nu}p_{\nu} \tag{2}$$

In the center-of-mass (CM) system, the total three-momentum before and after the reaction is zero:

$$\sum_{i}^{N} P_i = \sum_{j}^{M} P'_j = 0 \tag{3}$$

where N and M are the numbers of initial and final particles respectively. In the case of ATLAS experiment, the CM system coincides with the laboratory system.

Considering that the interacting beams are aligned in the z-direction, one can use the polar coordinate to express the moving direction of the outgoing particle. θ is the angle between the decay products and the beam axis, while the azimuthal angle ϕ is the angle in the transverse plane around the beam line. In experimental particle physics the *pseudo-rapidity*, η, is usually preferred to the polar angle when defining a measure of the angle between a particle and the beam axis. The reason is that the differences in the pseudo-rapidity is *Lorentz invariant* under boosts along the longitudinal axis.

$$\eta = -\ln(\tan(\frac{\theta}{2})) \tag{4}$$

For example, the $\eta = 0$ describes a particle moving perpendicular to the beam axis. Another important quantity is the angular separation of particles

$$\Delta R = \sqrt{\Delta\eta^2 + \Delta\phi^2} \tag{5}$$

For two interacting beams moving in the z-direction, the transverse momentum is zero. Because of the conservation of momentum principle, one expects a zero value for the final transverse momenta also. Any deviation from the expected value shows that some particles escape from the detector without leaving any track. The missing transverse energy is defined as

$$E_T^{miss} = \sqrt{M^2 + P_T^2} \tag{6}$$

where P_T is missing three-momentum transverse and M is the total mass of the escaping particles. The E_T^{miss} is an indirect way to detect neutrinos in a reaction. It is impossible to find the missing energy per particle in a reaction and therefore one should find the whole missing energy for the entire reaction.

3.2 Software

For this project the MadGraph5 generator has been used to generate the Monte Carlo (MC) sample events. The validation code is written in the C++ programming language. We also employ ROOT [15], which is a scientific software framework for big data processing.

3.3 Generation and Validation

Event generation is the first step in the event production chain. Some information about the reaction should be prepared in the generation file (job option) to result in the desired reaction and final states. In our case, the Higgs mass is set to 125 GeV/c^2 and all decay modes are turned off except for 4τ. We have also set other parameters like the LO trilinear Higgs self-coupling, the coupling of Higgs to other SM Higgs or top quarks. One can also put some limitations on the decay modes of τ or on the range of η or minimum transverse momentum.

Inside the validation code, one can check for the right particles in the final state with the correct four-momenta. For example, we check whether all events contain 2 Higgs bosons and 4τ. Histograms are then filled to study the kinematics of all involved particles in the reaction.

3.4 Objective

In this project, we are going to consider the non-resonant Higgs-pair production, which decays through $hh \to \tau\tau\tau\tau$. We generate the MC events for seven different trilinear Higgs self-couplings ($\lambda_{hhh} = 0, \pm1, \pm2, \pm10$) at Leading Order level, each one with 2000 events and then validate them. For example, $\lambda_{hhh} = 1$ corresponds to the SM Higgs self-coupling. We also validate the MC events for a *Next-to-Leading-Order* (NLO) simulation of $\lambda = 1$ to see how the correspondings histograms behave compared to the LO simulations of $\lambda_{hhh} = 1$. The NLO means that the vertices in the Feynman diagrams emerge from the NLO Lagrangian and each appropriate Feynman diagrams can contain vertices of order Q^4.

4 Results and Analysis

Fig. 2 shows two LO Feynamn diagrams resulting in di-Higgs production through gluon-gluon fusion. In general, the box-like diagram generates Higgs particles with higher transverse momentum while for the Higgs particles carrying smaller transverse momentum, the triangle diagram dominates.

For all plotted histograms in this section, the legends λ_i's mean $\lambda = i$, where $i = 0, \pm1, \pm2, \pm10$.

4.1 Histograms Analysis

Figs. 4 and 5 illustrate the angular distance of Higgs pairs in terms of ΔR and $\Delta\Phi$ respectively for different LO λ_{hhh} simulations. The histograms peak at 3.14 Rad which confirms that the Higgs particles emerge almost back-to-back. This is to be expected because of momentum conservation principle.

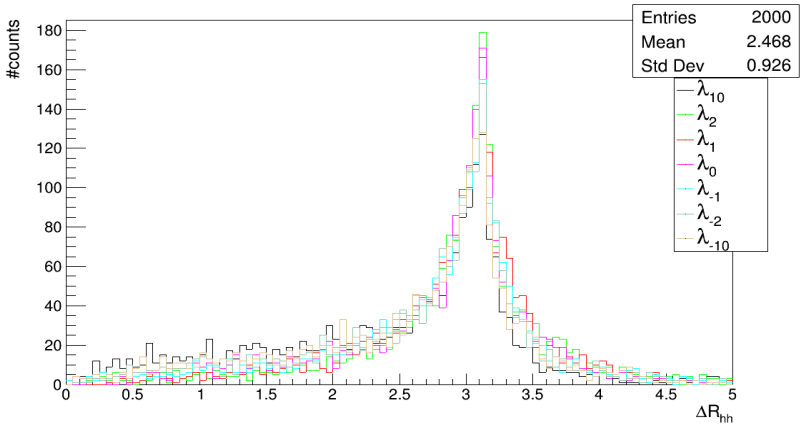

Figure 4: ΔR between Higgs particles for different LO λ_{hhh}.

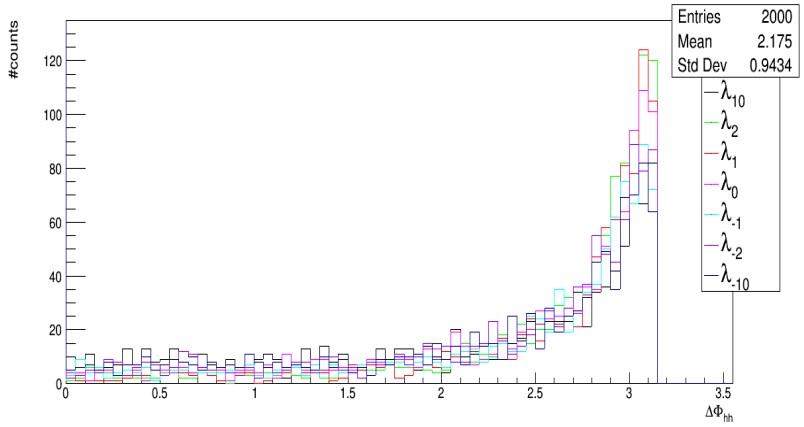

Figure 5: $\Delta\Phi$ between Higgs particles for different LO λ_{hhh}.

Fig. 6 and 7 show that in general, through the NLO $\lambda_{hhh} = 1$ simulation a higher number of Higgs particles emerge back to back compared to the LO $\lambda_{hhh} = 1$ simulation.

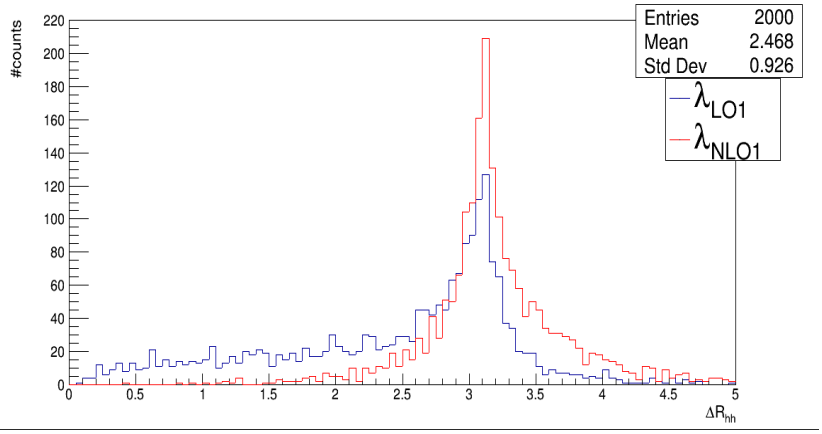

Figure 6: ΔR between Higgs particles for LO and NLO $\lambda_{hhh} = 1$.

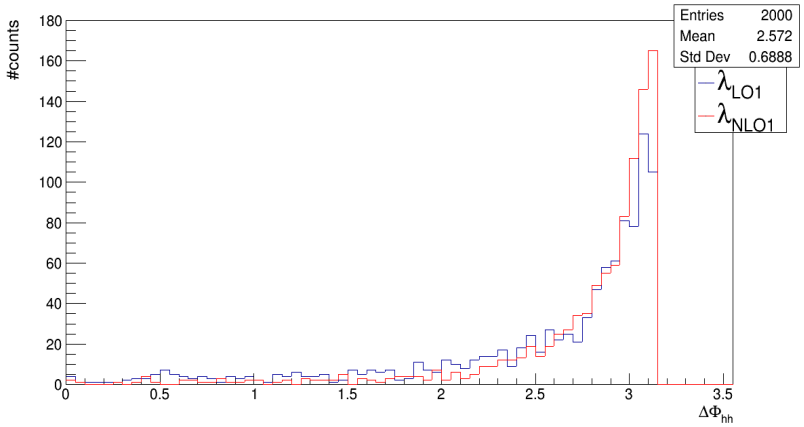

Figure 7: $\Delta\phi$ between Higgs particles for LO and NLO $\lambda_{hhh} = 1$.

The histograms of the Higgs transverse momentum have been plotted in the Fig. 8 for different LO λ_{hhh} simulations. While for $\lambda_{hhh} = 1, 2$ the box-like diagram dominates, for $\lambda_{hhh} = 0, -1, -2$ we have contributions of both triangle and box-like diagrams and the $\lambda_{hhh} = \pm 10$ contribute more toward the triangle diagram.

Fig. 9 shows that the Higgs samples extracted from the NLO λ_{hhh} simulation carry transverse momenta which are slightly higher than the LO simulated samples.

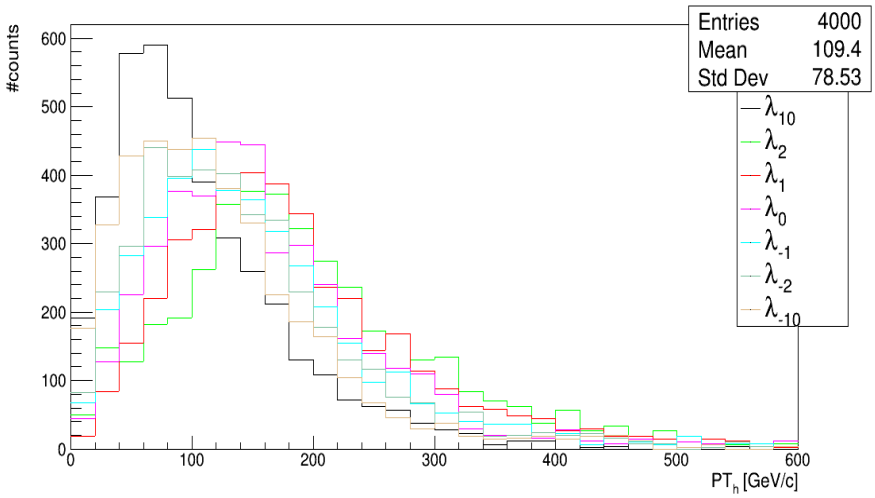

Figure 8: The Higgs transverse momentum for different LO λ_{hhh}.

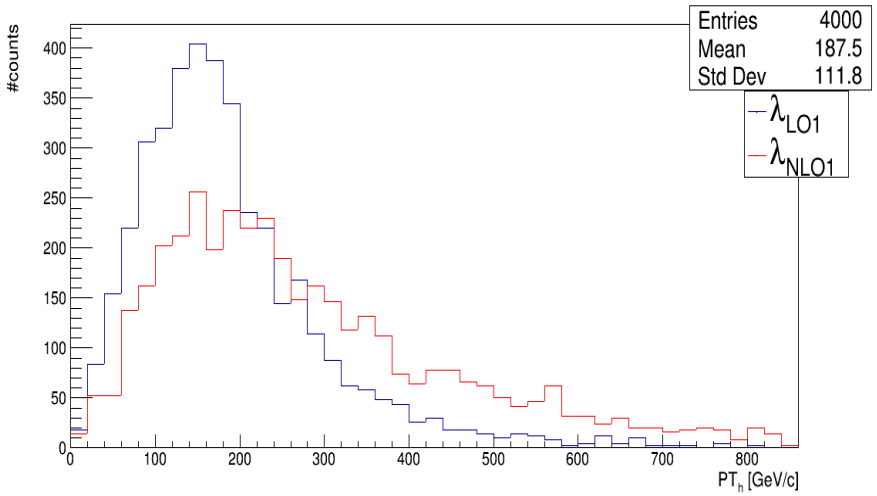

Figure 9: The Higgs transverse momentum for LO and NLO $\lambda_{hhh} = 1$.

Fig. 10 shows that the LO simulations of $\lambda_{hhh} = \pm 1, 0, 2$ lead to the higher di-Higgs mass compared to $\lambda_{hhh} = \pm 10, -2$ simulations. Additionally, from the NLO $\lambda_{hhh} = 1$ simulation, one gets larger values for di-Higgs mass in comparison with the LO $\lambda_{hhh} = 1$ simulation. Meanwhile we can not ignore that the NLO simulated samples give rise to a wider range of values for di-Higgs mass (see Fig. 11). One may conclude that the NLO $\lambda_{hhh} = 1$ and the LO $\lambda_{hhh} = \pm 1, 0, 2$ simulation produce more energetic Higgs pairs respectively. This can be confirmed by Figs. 12 and 13 representing the histograms of the Higgs-pair energies.

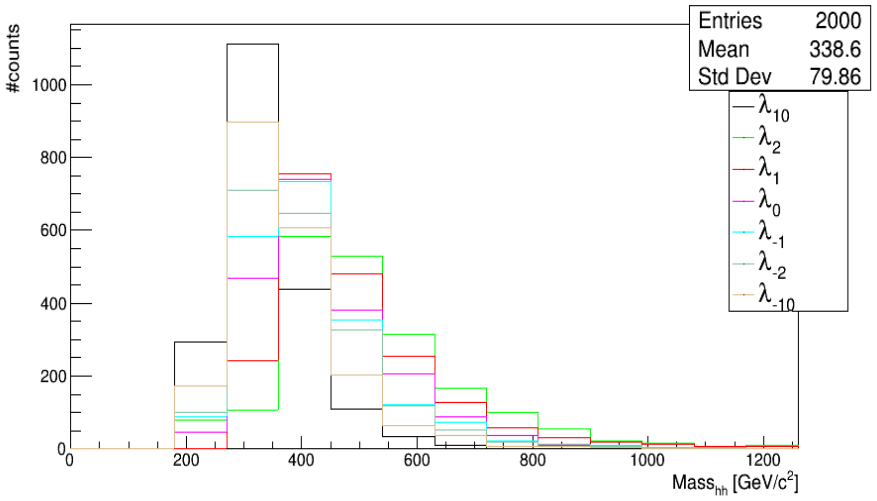

Figure 10: Di-Higgs mass for different λ_{hhh}.

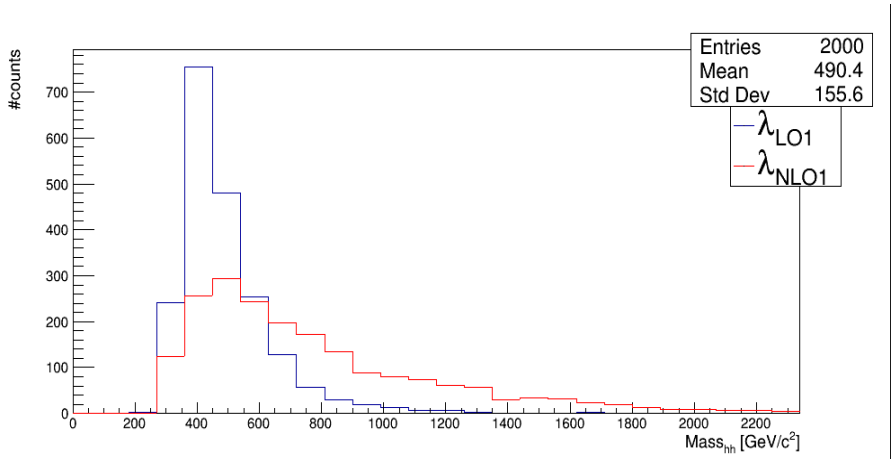

Figure 11: Di-Higgs mass for LO and NLO $\lambda_{hhh} = 1$.

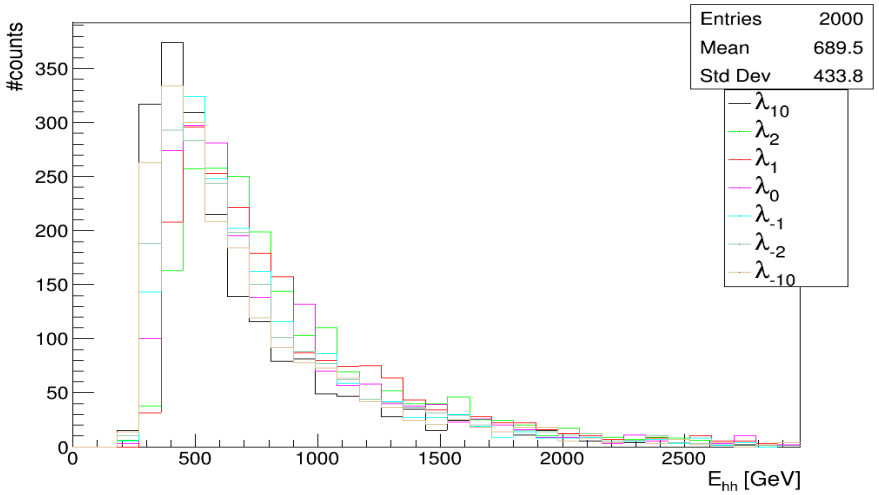

Figure 12: Di-Higgs energy for different LO λ_{hhh}.

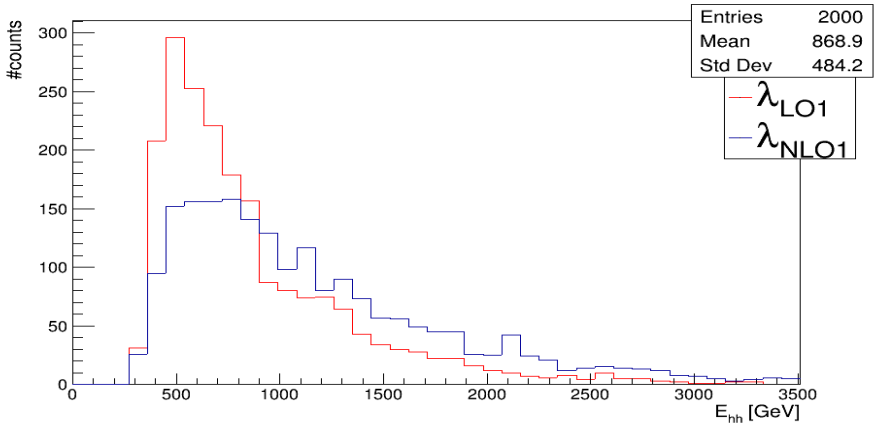

Figure 13: Di-Higgs energy for LO and NLO $\lambda_{hhh} = 1$.

Fig. 14 illustrates the transverse momenta of τ particles extracted from the LO λ_{hhh} simulation.

Although the tails of histograms show that a number of τ particles are produced with large transverse momenta, most of them carry smaller values. The Fig. 15 contains the histograms of τ transverse momenta for LO and NLO $\lambda_{hhh} = 1$ simulated data samples. The NLO simulation generates the τ particles with larger transverse momentum.

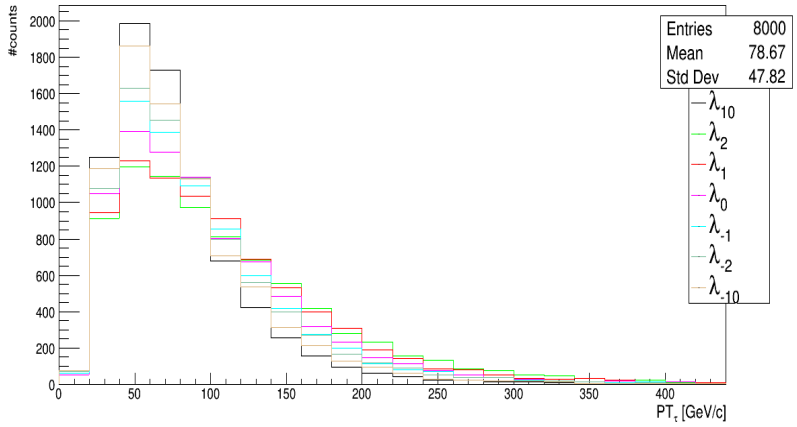

Figure 14: 4τ transverse momentum for different LO λ_{hhh}.

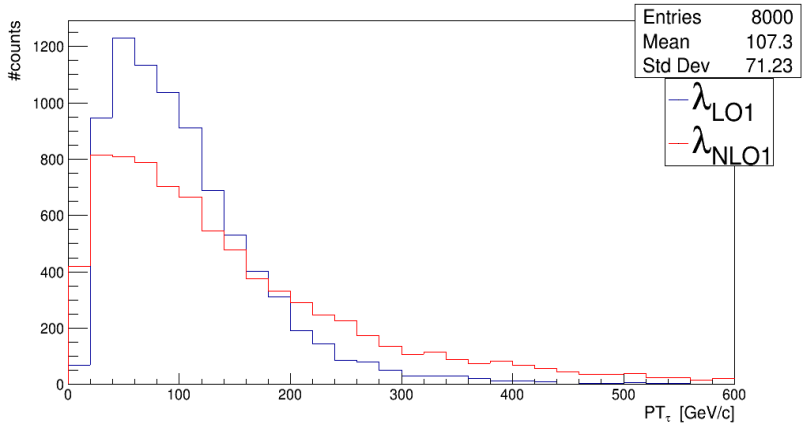

Figure 15: 4τ transverse momentum for LO and NLO $\lambda_{hhh} = 1$.

The τ particles coming from the same parent fly with a ΔR difference, which might differ depending on the value of λ_{hhh} (see Fig. 16). The Higgs particles with higher momentum decay to more collimated particles. Therefore, the triangle diagram, which is mostly from $\lambda_{hhh} = \pm 10$ simulation, produces more divergent products. The NLO trilinear Higgs self-coupling simulation leads to smaller deviation angle for τ particles compared to LO simulation because the Higgs bosons have higher transverse momenta(see Fig. 17).

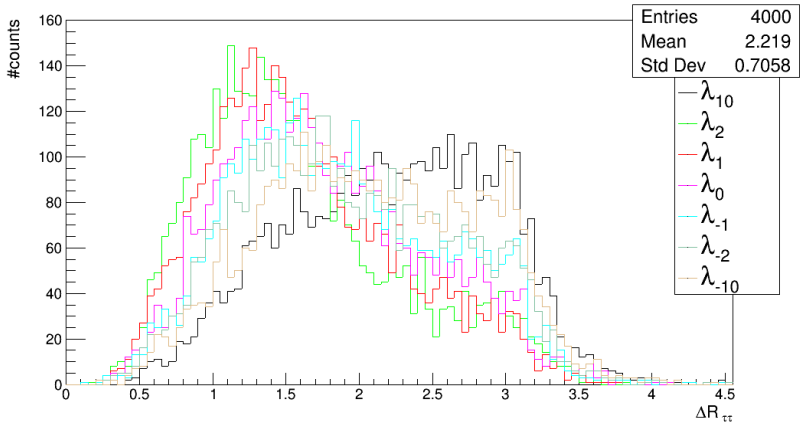

Figure 16: DR between two τs with the same parents for different values of λ_{hhh}.

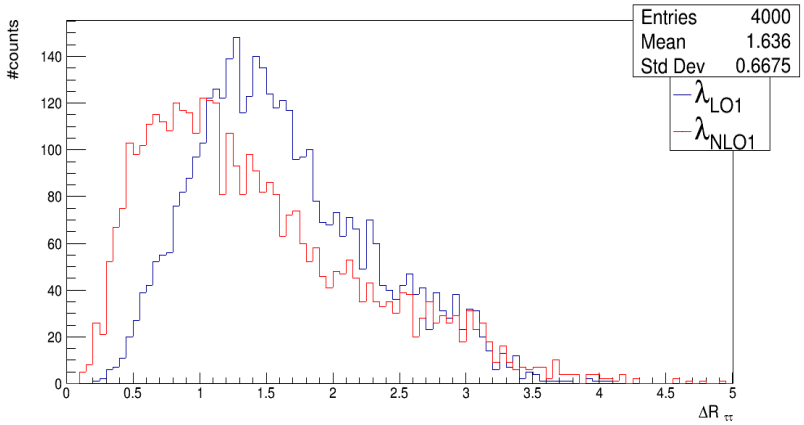

Figure 17: DR between two τs with the same parents for LO and NLO $\lambda_{hhh} = 1$.

Fig. 18 gives a numerical description of the missing transverse energy per event for the considered range of LO λ_{hhh}. The histograms show that among all λ_{hhh} simulations, the values which are closer to the SM expectation, lead to slightly more energetic neutrinos. Additionally, the missing energies of the NLO simulated samples for $\lambda_{hhh} = 1$ are higher than for the corresponding LO simulated samples (see Fig. 19). One can conclude that in general, the Higgs bosons with the higher transverse momenta result in final states with larger missing transverse energy.

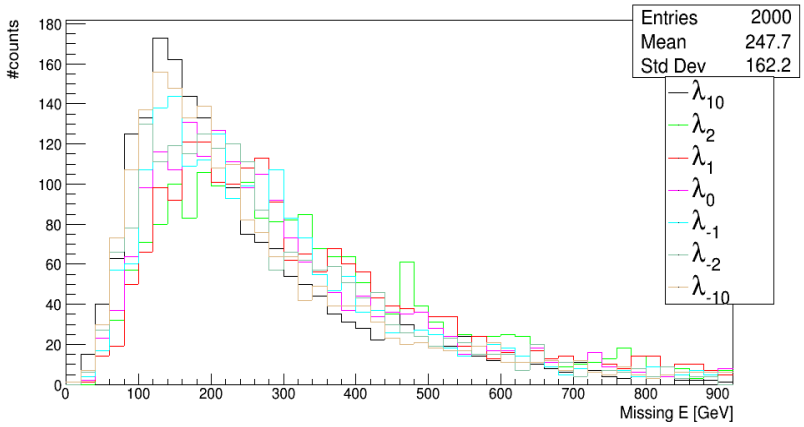

Figure 18: The missing energy per event for different value of λ_{hhh}.

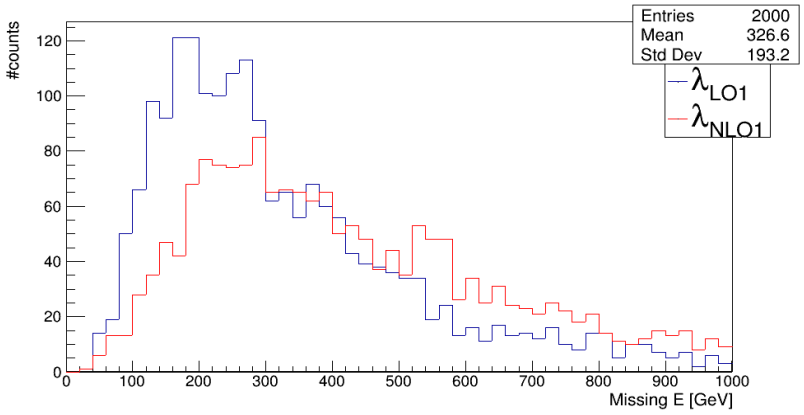

Figure 19: The missing energy per event for LO and NLO $\lambda_{hhh} = 1$.

5 Summary and Conclusion

The Higgs self-coupling has a vital role by giving a deeper understanding of the Higgs particle. Furthermore, the way it opens to physics beyond the SM, encourages us to do MC simulation studies for varying λ_{hhh}. In this project, we investigate the effects of choosing different values for λ_{hhh} on the kinematics of all particles involved in the $hh \to \tau\tau\tau\tau$ decay channel and the results are compared with what we get from the SM prediction of λ_{hhh}.

The data show that λ_{hhh} more close to the SM trilinear Higgs self-coupling results in generating the Higgs particles with the higher masses and higher momenta. On the other hand, for the more massive Higgs bosons we have more energetic neutrinos in the final states which escape from the detector without being detected.

References

[1] Steven Weinberg. A model of leptons. *Phys. Rev. Lett.*, 19:1264–1266, Nov 1967.

[2] Zhiliang Cao and Henry Gu Cao. Unified field theory and the configuration of particles. *International Journal of Physics*, 1(6):151–161, 2013.

[3] G. Aad et al. The ATLAS Experiment at the CERN Large Hadron Collider. *JINST*, 3:S08003, 2008.

[4] S. Chatrchyan et al. The CMS Experiment at the CERN LHC. *JINST*, 3:S08004, 2008.

[5] G. Aad, T. Abajyan, B. Abbott, and et al. Observation of a new particle in the search for the standard model higgs boson with the ATLAS detector at the LHC. *Physics Letters B*, 716(1):1 – 29, 2012.

[6] S. Chatrchyan et al. Observation of a new boson at a mass of 125 GeV with the CMS experiment at the LHC. *Physics Letters B*, 716(1):30 – 61, 2012.

[7] F. Englert and R. Brout. Broken symmetry and the mass of gauge vector mesons. *Phys. Rev. Lett.*, 13:321–323, Aug 1964.

[8] Vernon Barger, Lisa L. Everett, C.B. Jackson, and Gabe Shaughnessy. Higgs-pair production and measurement of the triscalar coupling at lhc(8,14). *Physics Letters B*, 728:433 – 436, 2014.

[9] Peter W. Higgs. Broken symmetries and the masses of gauge bosons. *Phys. Rev. Lett.*, 13:508–509, Oct 1964.

[10] El Hassan Saidi. On higgs self-coupling parameter λ of the standard model. *Nuclear Physics B*, 893:158 – 186, 2015.

[11] CMS Collaboration. Model independent search for Higgs boson pair production in the $\mathrm{b\bar{b}}\tau^+\tau^-$ final state. 2016.

[12] R. Frederix, S. Frixione, V. Hirschi, F. Maltoni, O. Mattelaer, P. Torrielli, E. Vryonidou, and M. Zaro. Higgs pair production at the lhc with nlo and parton-shower effects. *Physics Letters B*, 732:142 – 149, 2014.

[13] A. Denner, S. Heinemeyer, I. Puljak, D. Rebuzzi, and M. Spira. Standard Model Higgs-Boson Branching Ratios with Uncertainties. *Eur. Phys. J.*, C71:1753, 2011.

[14] C. et al Patrignani. Review of particle physics. *Chin. Phys.*, C40(10):100001, 2016 and 2017 update.

[15] I. Antcheva, M. Ballintijn, and B. Bellenot et al. Root — a C++ framework for petabyte data storage, statistical analysis and visualization. *Computer Physics Communications*, 180(12):2499 – 2512, 2009.